Iraqi Journal of Physics, 2024 *Vol. 22, No. 4, PP. 1-10*
https://doi.org/10.30723/ijp.v22i4.1280 *P-ISSN: 2070-4003*
E-ISSN: 2664-5548

Study the Influence of X-ray on the Optical and Mechanical Properties of CMC HV/ PAC LV Polymeric Films

Najla Ali Elgheryani [1a*]
[1]*Physics Department, Faculty of Education, University of Benghazi, Benghazi, Libya*
[a*]Corresponding author: nagla.elgerani@uob.edu.ly

Abstract

In this work, carboxymethyl cellulose/polyanionic cellulose (CMC HV/PAC LV) films were prepared and exposed to different X-ray doses (0, 200, 400, 600 and 800 cGy). Absorption and transmission measurements of the ultraviolet spectrum of the incident light were studied with a DU 800 spectrophotometer. Stress and strain were calculated by applying a tensile force to the samples and increasing its amplitude until the sample breaks. Applying this force to the samples increased the length of the samples. The absorption of CMC HV/PAC LV films increased with increasing X-ray dose, and therefore, the absorption coefficient increased with increasing X-ray dose. The results show that the amount of spectral transmittance of the films decreased with increasing X-ray dose, indicating that the opacity of the samples increased with increasing X-ray dose. The characteristic absorption peaks are observed at 275 nm^{-1}, 328 nm^{-1}, 345 nm^{-1}, 370 nm^{-1}, and 470 nm^{-1}, indicating molecular bonding. Increasing the X-ray dose decreases the elastic modulus of the films, and the stress amplification factor decreases with increasing strain ratio, indicating that X-ray photon irradiation leads to a decrease in the elasticity of the films. The results of this research may be useful in many fields, including industrial, medical or scientific research, as well as in oil fields.

Article Info.

Keywords:
Carboxymethyl, Polyanionic, UV-VIS Absorption, X-ray Doses, Stress.

Article history:
Received: May, 30, 2024
Revised: Aug. 01, 2024
Accepted: Aug. 18, 2024
Published: Dec.01,2024

1. Introduction

Cellulose, the most abundant biopolymer on Earth, is a high molecular weight linear polymer composed of glucose monosaccharide units interconnected by beta-acetal bonds. It exhibits unique characteristics due to hydrogen bonds in its molecular structure. Therefore, cellulose has limited solubility and resistance to melting in common solvents. Carboxymethyl cellulose (CMC) is a water-soluble anionic derivative of cellulose [1]. It is produced from cellulose by replacing some of its hydroxyl groups with carboxymethyl groups. Sodium carboxymethyl cellulose is the sodium salt form of carboxymethyl cellulose. It is produced from natural cellulose by etherification, where sodium groups replace hydroxyl groups. It is a linear, semi-flexible, negatively charged polyelectrolyte. Due to its availability and its thickening and swelling properties, sodium carboxymethylcellulose (NaCMC) is used in many industries. Application areas include pharmaceutical, personal care, household products, food, water treatment, mineral processing, paints and paper industries [2].

Polyanionic cellulose, water-soluble biopolymer, is chemically modified from cellulose by introducing anionic reagents, such as carboxymethyl groups, to introduce negative charges along the polymer chain. This modification enhances its water solubility and makes it useful in various industrial applications. Polymer properties such as viscosity and molecular weight can be tailored by substituting other functional groups in the chain [3]. Polyanionic cellulose (PAC), dissolved in distilled water, is used as a drilling fluid substitute in cuttings transport studies or other multiphase flow studies relevant to the oil and gas industry [3].

The absorption or reflection spectroscopy of the ultraviolet and near visible parts of the electromagnetic spectrum is known as UV spectroscopy. This method is used in many scientific and applied fields due to its ease of implementation[4]. The UV-visible spectrum results from the interaction of electromagnetic radiation in the UV-visible region with ions, atoms or molecules. It forms the basis for the analysis of inorganic and organic materials and biomolecules [5]. UV radiation has a wavelength between 200 and 400 nm and is responsible for discoloration, corrosion, loss of gloss and cracking of polymer materials. The physical and chemical changes that occur during photo-oxidation reactions are characterized by an increase in the concentration of oxygen-containing groups, which attack the bonds in the polymer molecules, thus reducing the length of the molecular chain [6]. Radiation can be ionizing or non-ionizing, depending on the energy of the irradiated sources. It includes X-rays from medical examinations, as well as X-rays from mesons, positrons, neutrons and other particles that form secondary cosmic rays produced after the interaction of primary cosmic rays with the Earth's atmosphere [7]. X-rays are, in general, the most common form of electromagnetic radiation. Advances in imaging technology have allowed for increasingly powerful and guided X-rays, as well as greater use of visible light in microbial and structural tissues of young material elements such as concrete [8]. The interaction of photons with matter is characterized by the fact that each X-ray photon is individually removed from the incident beam in a single event. The X-ray photon collides with one of the electrons of the absorbing element and no energy is lost. In the collision process, the scattered radiation will retain the same wavelength as the incident beam [9]. X-rays have become a long-standing complement to gamma rays due to the many similarities between the two photon-based technologies. Many changes are considered when migrating to X-rays, including the dose rate effect, the effect on materials, temperature impacts, processing time, and any possible induced radioactivity [10].

Absorption spectroscopy is a powerful technique to study photoinduced phenomena in a wide range of states, from solutions to solid film samples. It was designed and developed based on photoinduced absorption changes or on the fact that photoexcitation triggers a chain of reactions with intermediate states or reaction steps with presumably different absorption spectra [11].

Ultraviolet and visible light -NIR absorption spectroscopy is one of the most popular measurement methods, among the most relevant advantages is the direct measurement, which requires little or no sample preparation, so the analysis is simple, fast and does not require manual intervention. It is a non-destructive analysis that uses a small amount of sample, being highly compatible with industrial use thanks to the compact instruments [12].

Polymers are safe, economical, have eco-sustainable properties and have many applications in engineering and scientific studies. Polymers can be used in optoelectronics, solar cells, UV filters, coatings, photovoltaics, light-emitting diodes, laser production and many other applications [13]. The mechanical properties of a polymer are one of the characteristics that distinguish it from small molecules, and which involve its behavior under stress. Stress-strain tests are the most widely used mechanical tests, but probably the least understood in terms of interpretation. In stress-strain tests, the sample is deformed at a constant rate and the stress required for this deformation is measured simultaneously [14]. Polymers exhibit a wide range of mechanical behaviors depending on the loading rate and temperature. The neglected aspect is relaxation, which is important because it acts over a wide time interval and starts as soon as the polymer is loaded [14]. The elastic modulus is the ratio of stress to strain in the linear elastic region and measures the stiffness of the material. The yield

stress is the stress at the end of the elastic region where the deformation can be reversed, i.e., the material returns to its original state [15]. Abd et al. reported that the absorbance and reflectivity value increase and the transmittance decrease as the solution concentration increases before and after irradiation [16]. Iqbala et al. samples irradiated with different X-ray fluences; irradiation enhanced the absorption in the UV-visible region [17]. Nouh et al. Samples of polyester polymer sheets were exposed to X-rays. Stress and strain measurements indicated that X-ray irradiation in the dose range of 30 to 100 kGy produced a highly resistant cross-linked polyester [18]. Hamza and Sharada A sample of polyvinyl alcohol doped with 5 wt% molybdenum oxide was prepared forming a composite film (PVA-MoO3) and exposed to UV radiation. The transmittance and oscillator energy decreased with increasing radiation exposure time. Furthermore, the results showed that the composite film (PVA-MoO3) can be used as a UV sensor [19]. Abdullahi et al. Tris-(8-hydroxyquinoline) aluminum exposed to different X-ray doses in the range of 5 to 20 Gy. The systematic changes observed in the optical properties of Alq3 and the resulting excellent linear response curves of irradiation doses as a function of signal intensities were encouraging [20]. Qwasmeh et al. They studied the effect of gamma radiation on the optical properties of polyethylene oxide thin films doped with different concentrations of potassium iodide (KI) salt. The optical properties of the thin films were found to be significantly influenced by the concentration of the KI dopant and gamma irradiation [21].

2. Materials and Methods

2. 1. Materials and Samples preparation

High-viscosity carboxymethyl cellulose (CMC HV) and low-viscosity polyanionic cellulose (PAC LV) were obtained from National Oil Corporation Jowfe Oil Technology/Ganfouda/Benghazi/Libya.

CMC HV / PAC LV films were prepared by mixing 73% CMC HV with 27% PAC LV to form films (the higher proportion of PAC LV gives a homogeneous film) using the casting technique. The mixture was dissolved in 40 ml distilled water for three hours at room temperature (30 °C) with stirring. The solution was poured onto a flat glass plate of 8cm diameter and allowed to dry at room temperature. A film was produced of a thickness varying between 49 and 50μm.

2. 2. Irradiation of samples:

CMC HV/PAC LV films were exposed to different X-ray doses (0, 200, 400, 600 and 800 cGy) provided from the X-ray facility of the National Cancer Center in Benghazi, Libya.

2. 3. Measurements

2. 3. 1. UV- Vis Spectra

Absorption and transmission measurements were studied using **a** UV-Vis spectrophotometer (DU 800, serial number 8000770, software version "2.0, Build 67"), firmware version 2.0.012, method name "Default Method" located in the laboratory of the Faculty of Sciences, Omar Al-Mukhtar University, Al-Bayda, Libya.

The absorption coefficient (α) was calculated using Eq. (1), where T is the transmittance value and d is the thickness of the sample [22]. The extinction coefficient (K) was calculated using Eq. (2), where λ is the wavelength of the incident photons [23]:

$$\alpha = -\frac{1}{d} \ln (T) \qquad (\mathbf{1})$$

$$K = \frac{\alpha \lambda}{4 \pi} \quad (2)$$

2. 3. 2. Mechanical Properties

Force (F) was applied on the to the 5 cm long and 1 cm wide CMC HV / PAC LV film samples shown in Fig. 1, and the tensile stress (σ_s) was calculated using Eq. (3) [24]:

$$\sigma_s = \frac{F}{A} \quad (3)$$

where (A) is the cross section of the samples.

Strain ($\boldsymbol{\varepsilon}$) was calculated from Eq. (4), [24]:

$$\varepsilon = \frac{(L - L_0)}{L_0} \quad (4)$$

where: L_0 is the original length of the sample and L is the changed length of the samples after applying the force.

The elastic modulus (E), which is a correlation between stress and strain, was calculated using Eq. (5) [24]:

$$E = \frac{\sigma_s}{\varepsilon} \quad (5)$$

The dependence of the stress-strain relationship for the different samples is given by:

$$\frac{\sigma_s}{2(\tau - \tau^{-2})} = C_1 + C_2 \tau^{-1} \quad (6)$$

where $\boldsymbol{\tau}$ is the stretch ratio ($\boldsymbol{\tau}$ = 1+ε), C_1 is a quantity relative to the ideal elastic behavior and C_2 expresses the deviation from the ideal elastic behavior [25-27].

Figure 1: CMC HV/PAC LV film.

3. Results and Discussion

3. 1. Ultraviolet and Visible Spectra

Fig. 2 shows the UV–visible spectra of CMC HV/CMC PAC LV films, which show the relationship between nanometer wavelength and UV–visible absorption for both irradiated and non-irradiated samples. The absorption of the spectra increased with increasing X-ray irradiation dose. The absorption peaks of CMC HV/PAC LV spectra were observed at 275 nm^{-1}, 328 nm^{-1}, 345 nm^{-1}, 370 nm^{-1}, 470 nm^{-1} [28, 29]. The UV absorption spectra of o-hydroxybenzophenone derivatives (C_{13}–H_{10}–O_2) essentially

retain the character of C_{13}–H_{10}–O_2 spectrum. Beta-carotene ($C_{40}H_{56}$) absorbs throughout the ultraviolet region, but particularly in the visible region between 400 and 500 nm with a peak at 470 nm [29].

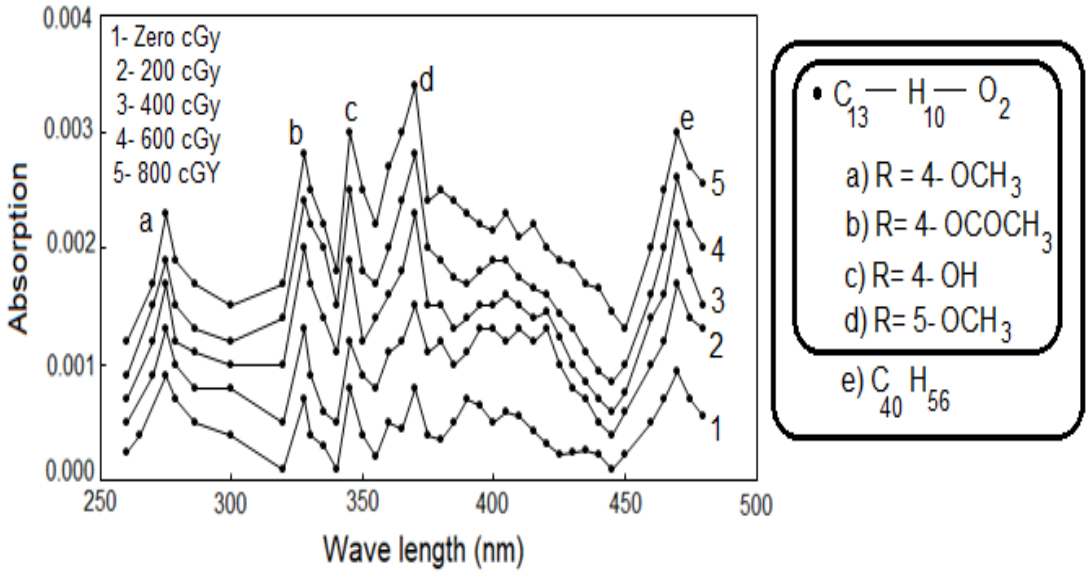

Figure 2: UV-Vis absorption spectra for all CMC HV/ PAC LV films.

Irradiation of the films with X-ray photons made them opaquer. Fig. 3 clearly shows that when the radiation dose increases, the spectral transmittance in the samples decreases.

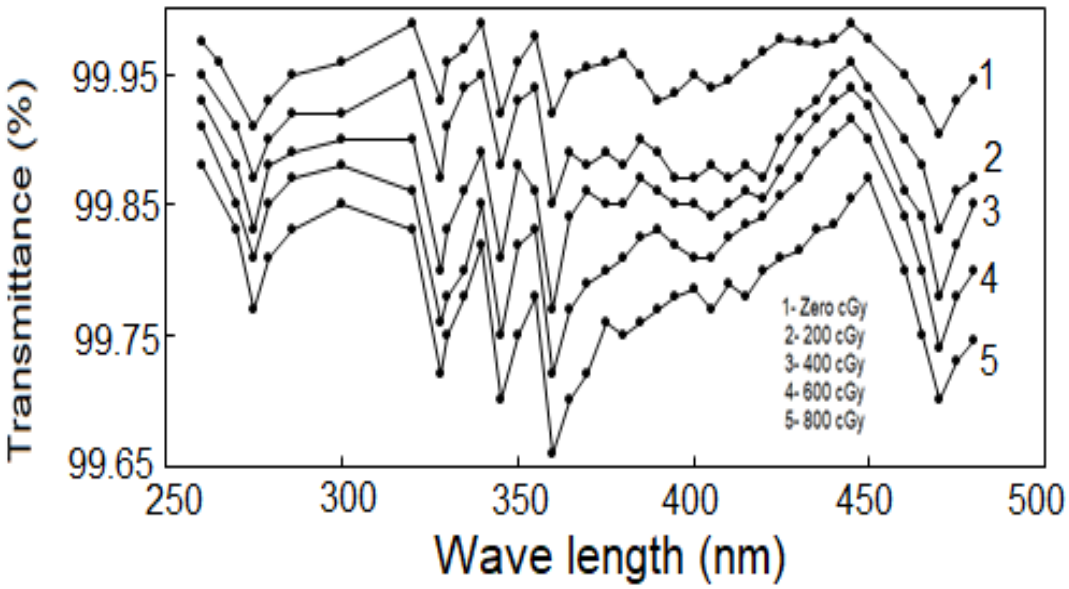

Figure 3: UV-visible transmittance spectra for all CMC HV/PAC LV films.

Fig. 4 shows the variation of the absorbance measured at the absorption peaks wavelengths (275, 328, 345, 370, 470 nm^{-1}) with the X-ray doses. It can be seen from Fig. 3 that the intensity of all molecular bonds increased with increasing X-ray doses. However, the absorption intensity of the spectrum at C_{40} H_{56}, C_{13} –H_{10} – O_2 (R = 5-OCH3), C_{13} –H_{10} – O_2 (R = 4- OH), C_{13} –H_{10} – O_2 (R = 4- $OCOCH_3$) and C_{13} –H_{10} – O_2 (R = 4- OCH_3) bonds increased with increasing the X-ray doses.

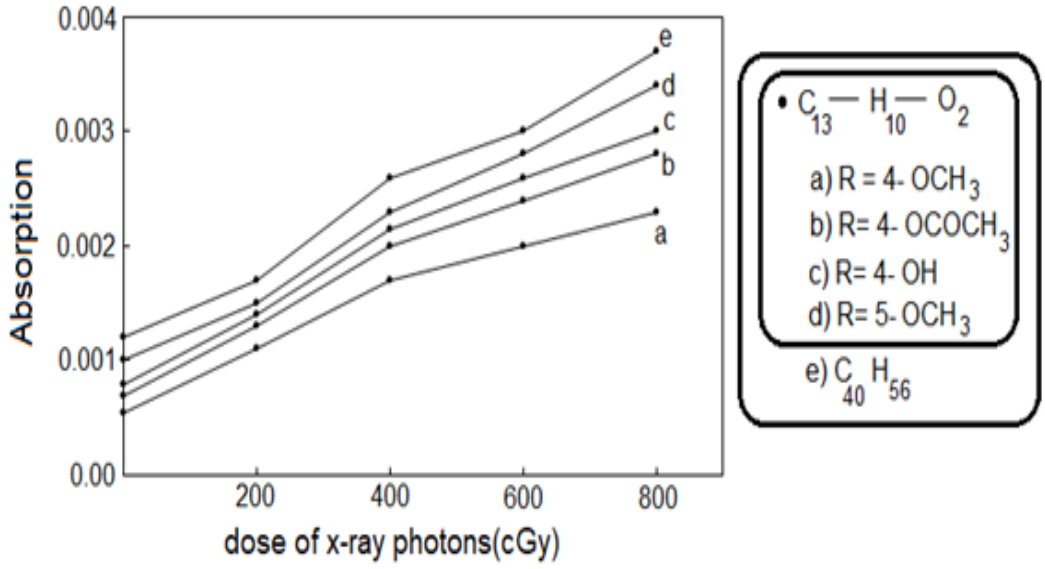

Figure 4: Variation of absorption measured at the absorption peaks wavelengths with X-ray doses.

The absorption coefficients of the UV-Vis spectrum for the different X-ray doses at the absorption peaks wavelengths are shown in Table 1; it is evident that the absorption coefficient increased with increasing the X-ray dose.

Table 1: The absorption coefficients of the UV-Vis spectrum with the X-ray doses at the absorption peaks wavelengths.

λ(nm)	Absorption coefficient α (mm^{-1})				
	0.0 cGy	**200 cGy**	**400 cGy**	**600 cGy**	**800 cGy**
275	0.018008	0.030023	0.034029	0.038036	0.046053
328	0.014005	0.026017	0.04004	0.048058	0.056079
345	0.016006	0.024014	0.038036	0.050063	0.06009
360	0.016006	0.030023	0.046053	0.056079	0.068116
470	0.019009	0.02802	0.044048	0.052068	0.06009

The extinction coefficients of the ultraviolet-visible spectra for the different X-ray doses at absorption peaks wavelengths are shown in Table 2; the extinction coefficient increased with increasing the X-ray dose.

Table 2: The extinction coefficient of the UV-Vis spectrum with the X-ray doses at the absorption peaks wavelengths.

λ(nm)	Extinction coefficient K (X 10^{-7})				
	0.0 cGy	**200 cGy**	**400 cGy**	**600 cGy**	**800 cGy**
275	3.94108	6.57351	7.45062	8.32795	10.0833
328	3.65736	6.79425	10.4563	12.5502	14.6448
345	4.39655	6.5962	10.4478	13.7514	16.5056
360	4.58771	8.60532	13.1999	16.0736	19.5237
470	7.11324	10.4852	16.4829	19.484	22.4859

3. 2. Mechanical Properties

Fig. 5 shows the effect of the X-ray dose on the stress-strain curves of CMC HV/PAC LV films. It can be observed that the slope, which is the value of the elastic modulus, of the stress-strain curves decreased with the increase of the X-ray dose; this

result is clearly shown in Fig. 6. The elastic modulus decreased with increasing the radiation dose. It can then be concluded that X-rays reduce the elasticity of the samples.

Fig. 7 shows the stress amplification factor ($\sigma/(2(\tau - \tau^{-2})$) plotted against the stress ratio (τ^{-1}). From these plots, the constants C_1 and C_2 can easily be determined. C_1 is determined from the intersection of the curves with the vertical coordinate and C_2 from the slope of the curves. The dependence of C_1 and C_2 on the X-ray dose is shown in Table 3. The behavior of C_1 and C_2 with CMC HV/PAC LV thin films samples may be due to network cross-links and other network defects [30].

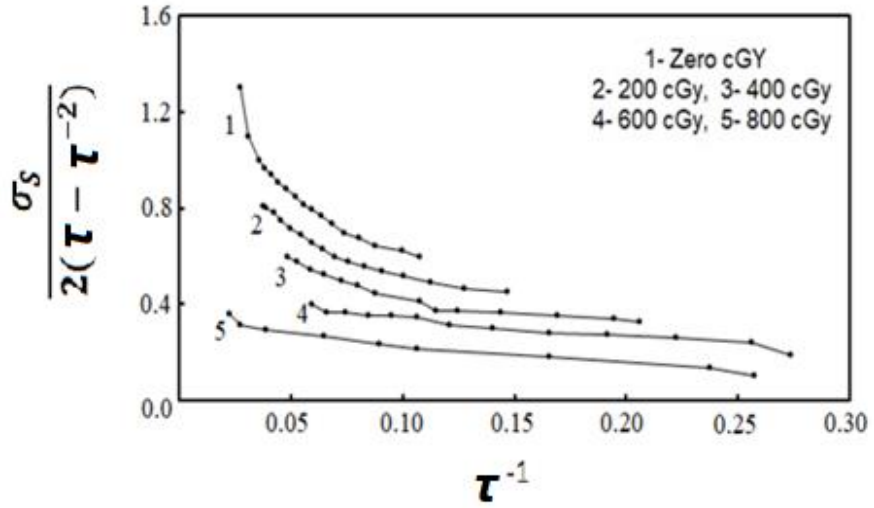

Figure 5: Stress- Strain curves for CMC HV/ PAC LV films for the different X- ray doses.

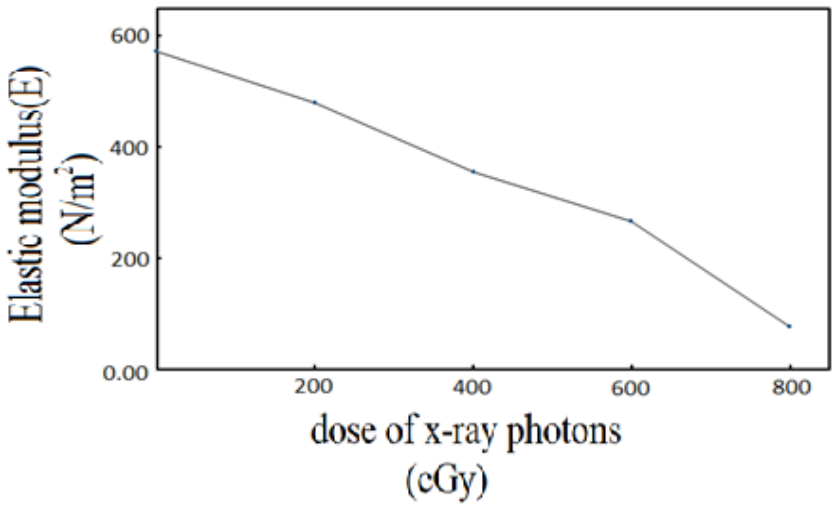

Figure 6: The effect of the different X-ray doses on the elastic modulus of CMC HV/ PAC LV thin films.

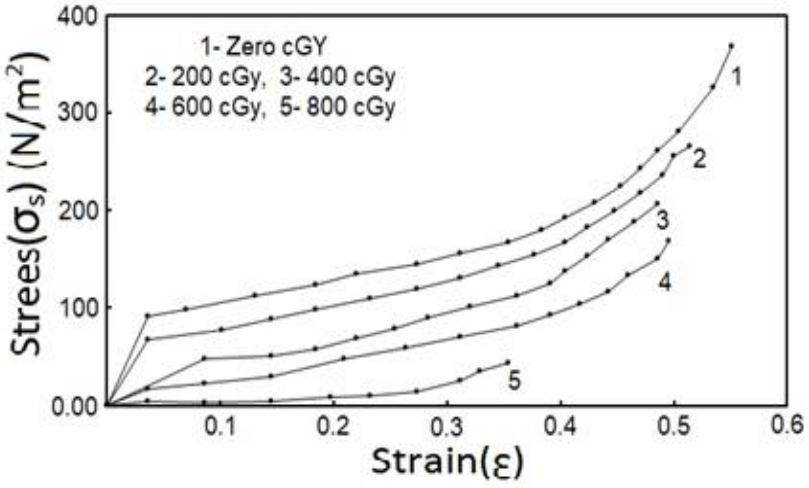

Figure 7: Strain amplification factor curve for CMC HV/ PAC LV films at different X-ray doses.

Table 3: The values of constant C_1 and C_2 for different X-ray doses for CMC HV/ PAC LV films.

Dose (cGy)	C_1	C_2
0	1.587714	-0.60039
200	1.177666	-0.44973
400	0.828006	-0.319
600	0.577972	-0.22347
800	0.421288	-0.17605

4. Conclusions

The UV-Vis spectra showed that absorption of the CMC HV/PAC LV films increased, and the transmittance decreased with the increase of the X-ray irradiation dose. So the absorption coefficient and extinction coefficient increased with increasing X-ray irradiation dose. The decrease in transmittance indicates an increase in the opacity of the samples with increasing the X-ray dose.

The increase in the X-ray dose caused a decrease in the elastic modulus and the stress amplification factor and an increase in the deformation ratio of the CMC HV/PAC LV films, indicating that X-ray irradiation leads to a decrease in the elasticity of CMC HV/PAC LV films. The results of this research may be useful in many fields, including industrial, medical, scientific, and petroleum research.

Acknowledgment

I would like to express my sincere thanks and gratitude who helped me carry out this research to Jowfe Oil Technology National Petroleum Corporation, especially Mr. Mohammad Bograd and Mr. Jamal Mohammad Al-Farjani, Ms. Ibtisam Al-Mazoghi and Mr. Ehab El-Boury from the National Cancer Center in Benghazi, Libya. Lastly, Saleha Thaoud Youssef and Salah Saleh Basil are staff members of the Physics Department at Omar Al-Mukhtar University, Al-Bayda, Libya.

Conflict of interest

Authors declare that they have no conflict of interest.

References

1. T. Churam, P. Usubharatana, and H. Phungrassami, Sustainability **16**, 2352 (2024). DOI: 10.3390/su16062352.
2. J. S. Behra, J. Mattsson, O. J. Cayre, E. S. J. Robles, H. Tang, and T. N. Hunter, ACS Appl. Poly. Mat. **1**, 344 (2019). DOI: 10.1021/acsapm.8b00110.
3. A. Busch, V. Myrseth, M. Khatibi, P. Skjetne, S. Hovda, and S. T. Johansen, Appl. Rheo. **28**, 201825154 (2018). DOI: 10.3933/applrheol-28-25154.
4. S. W. C. Shabbir, Shilpi Int. J. of Pharm. Sci. **2**, 1232 (2024). DOI: 10.5281/zenodo.12570882.
5. T. R. Sneha, R. Sheeja, and V. M. Nishad, Int. J. Pharm. Res. Appl. **7**, 532 (2022). DOI: 10.35629/7781-0702532535.
6. P. K. Kamweru, F. G. Ndiritu, T. Kinyanjui, Z. W. Muthui, R. G. Ngumbu, and P. M. Odhiambo, Int. J. Phys. Sci. **9**, 545 (2014). DOI: 10.5897/IJPS2014.4229
7. N. Karmaker, K. M. Maraz, F. Islam, M. M. Haque, M. Razzak, M. Mollah, M. Faruque, and R. A. Khan, GSC Advan. Res. Rev. Mod. Phys. **7**, 064 (2021). DOI: 10.30574/gscarr.2021.7.1.0043.
8. S. Prabhu, D. K. Naveen, S. Bangera, and B. S. Bhat, Journal of Physics: Conference Series (Mangalore, India IOP Publishing, 2020). p. 012036.
9. G. Alcocer, Mediterr. J. Bas. Appl. Sci. (MJBAS) **5**, 51 (2022). DOI: 10.46382/MJBAS.2021.5406.
10. B. Mcevoy, A. Maksimovic, D. Howell, P. Reppert, D. Ryan, N. Rowan, and H. Michel, Rad. Phys. Chem. **208**, 110915 (2023). DOI: 10.1016/j.radphyschem.2023.110915.
11. H. P. Pasanen, R. Khan, J. A. Odutola, and N. V. Tkachenko, J. Phys. Chem. C **128**, 6167 (2024). DOI: 10.1021/acs.jpcc.4c00981.
12. D. Boskou, *Olive Oil: Constituents, Quality, Health Properties and Bioconversions* (Rijeka, IntechOpen, 2012).
13. H. Elhosiny Ali, M. Abdel-Aziz, A. Mahmoud Ibrahiem, M. A. Sayed, H. S. M. Abd-Rabboh, N. S. Awwad, H. Algarni, M. Shkir, and M. Yasmin Khairy, Polymers **14**, 1741 (2022). DOI: 10.3390/polym14091741.
14. T. Commins and C. R. Siviour, Proce. Roy. Soci. **479**, 20220830 (2023). DOI: 10.1098/rspa.2022.0830.
15. R. H. Alasfar, S. Ahzi, N. Barth, V. Kochkodan, M. Khraisheh, and M. Koç, Polymers **14**, 360 (2022). DOI: 10.3390/polym14030360.
16. A. N. Abd, S. K. Rahi, and Z. M. A. Khalik, NeuroQuantology **18**, 21 (2020). DOI: 10.14704/nq.2020.18.6.NQ20178.
17. S. Iqbal, M. S. Rafique, S. Anjum, A. Hayat, and N. Iqbal, Appl. Surf. Sci. **259**, 853 (2012). DOI: 10.1016/j.apsusc.2012.07.146.
18. S. A. Nouh, H. A. El-Nabarawy, M. M. Abutalib, and R. A. Bahareth, Eur. Phys. J. Appl. Phys. **62**, 30201 (2013). DOI: 10.1051/epjap/2013130050.
19. M. Hamza, Libyan J. Sci. **25**, 10 (2022).
20. S. Abdullahi, A. Aydarous, and N. Salah, Radiation Phys. Chem. **188**, 109656 (2021). DOI: 10.1016/j.radphyschem.2021.109656.
21. A. a. H. Qwasmeh, B. A. Abu Saleh, M. Al-Tweissi, M. a. A. Tarawneh, Z. M. Elimat, R. I. Alzubi, and H. K. Juwhari, J. Compos. Sci. **7**, 194 (2023). DOI: 10.3390/jcs7050194.
22. R. Dewi, Krisman, Zulkarnain, Rahmawati, and T. S. L. Husain S., AIP Conf. Proce. **2169**, 060002 (2019). DOI: 10.1063/1.5132680.
23. A. Axelevitch, B. Gorenstein, and G. Golan, Phys. Proce. **32**, 1 (2012). DOI: 10.1016/j.phpro.2012.03.510.
24. F. P. Beer, E. R. Johnston, J. T. Dewolf, and D. F. Mazurek, *Mechanics of Materials* (New York, McGraw-Hill, 2012).
25. M. Konarzewski, M. Stankiewicz, M. Sarzyński, M. Wieczorek, M. Czerwińska, P. Prasuła, and R. Panowicz, Acta Mech. Autom. **17**, 317 (2023). DOI: 10.2478/ama-2023-0037.
26. X. Liang and A. J. Crosby, Ext. Mech. Lett. **35**, 100637 (2020). DOI: 10.1016/j.eml.2020.100637.
27. P. Sotta, P.-A. Albouy, M. Abou Taha, B. Moreaux, and C. Fayolle, Polymers **14**, 9 (2022). DOI: 10.3390/polym14010009.
28. D. Lingegowda, J. Kumar, A. Prasad, M. Z. Mahsa Zarei, and S. G. Shubha Gopal, Romanian J. Biophys. **22**, 137 (2012).
29. R. A. Pratiwi and A. B. D. Nandiyanto, Indonesian J. Educ. Res. Tech. **2**, 20 (2022). DOI: 10.17509/ijert.v2i1.35171.
30. S. S. Hamza, S. El-Sabbagh, and F. Shokr, Int. J. Poly. Mat. Poly. Biomat. **57**, 203 (2008). DOI: 10.1080/00914030701413330.

تأثير فوتونات الأشعة السينية على بعض الخواص البصرية والميكانيكية للأغشية الرقيقة CMCHV/ PACLV

نجلاء علي الغرياني[1]
[1]قسم الفيزياء، كلية التربية، جامعة بنغازي، بنغازي، ليبيا

الخلاصة

تم إعداد الأغشية الرقيقة CMC HV/PAC LV في هذا البحث وتعريضها لجرعات مختلفة من فوتونات الأشعة السينية (0، 200، 400، 600، و800 cGy). تم دراسة امتصاص ونفاذ طيف الأشعة فوق البنفسجية الساقطة باستخدام مقياس الطيف الضوئي DU 800. تم حساب الإجهاد والانفعال من نتائج قياسات القوى المطبقة على العينات والزيادة في طول العينات. تزداد كمية الطيف الممتص مع زيادة جرعة الأشعة السينية للأغشية الرقيقة CMC HV/PAC LV وبالتالي يزيد معامل الامتصاص مع زيادة جرعة الأشعة السينية. ومن النتائج لوحظ أن كمية النفاذية الطيفية للأغشية الرقيقة تتناقص مع زيادة جرعة الأشعة السينية، مما يدل على أن عتامة العينات تزداد مع زيادة جرعة الأشعة السينية. يتم ملاحظة قمم الامتصاص المميزة عند $275nm^{-1}$، $328\ nm^{-1}$، $345\ nm^{-1}$، $370\ nm^{-1}$، $470\ nm^{-1}$ مما يشير إلى الترابط الجزيئي، كما أن زيادة جرعة الأشعة السينية أدت إلى انخفاض معامل مرونة الأغشية الرقيقة، وعامل تضخيم الإجهاد يتناقص مع زيادة نسبة الانفعال، مما يشير إلى أن تشعيع الفوتون السينية يؤدي إلى انخفاض مرونة الأغشية الرقيقة. ويمكن أن تكون نتائج هذا البحث مفيدة في العديد من المجالات، بما في ذلك البحوث الصناعية أو الطبية أو العلمية، وكذلك في مجالات النفط.

الكلمات المفتاحية: كربوكسي ميثيل، بولي أنيون، امتصاص الأشعة فوق البنفسجية والمرئية، الإجهاد، جرعات الأشعة السينية.